Pavel, Ileana-Alexandra et al., 2017. Effect of Meso vs Macro Size of Hierarchical Porous Silica on the Adsorption and Activity of Immobilized β-Galactosidase. Langmuir, 33(13), pp.3333–3340.

LANGMUIR

Article

Effect of meso vs macro-size of hierarchical porous silica on the adsorption and activity of immobilized #-galactosidase

Ileana-Alexandra Pavel, Sofia F. Prazeres, Gemma Montalvo, Carmen Garcia-Ruiz, Vincent Nicolas, Alain Celzard, Francois Dehez, laetitia CANABADY-ROCHELLE, Nadia Canilho, and Andreea Pasc

Langmuir, **Just Accepted Manuscript** • DOI: 10.1021/acs.langmuir.7b00134 • Publication Date (Web): 16 Mar 2017

Effect of meso *vs* macro-size of hierarchical porous silica on the adsorption and activity of immobilized β-galactosidase

Ileana-Alexandra Pavel,[a‡] Sofia F. Prazeres, [b‡] Gemma Montalvo,[b,c] Carmen Garcia Ruiz,[b,c] Vincent Nicolas,[d] Alain Celzard,[d] François Dehez,[a] Laetitia Canabady-Rochelle,[e] Nadia Canilho,[a*] Andreea Pasc[a*]

[a]SRSMC UMR 7565 CNRS-Université de Lorraine, Bvd des Aiguillettes, BP 70239, F-54506 Vandoeuvre-lès-Nancy, France, [b]Department of Analytical Chemistry, Physical Chemistry and Chemical Engineering, University of Alcala, E-28871 Alcala de Henares, Spain, [c] University Institute of Research in Police Sciences (IUICP), E-28871 Alcalá de Henares (Madrid) Spain, [d]Institut Jean Lamour UMR 7198 CNRS – Université de Lorraine, ENSTIB, 27 rue Philippe Séguin, CS 60036, 88026 Epinal cedex, France, [e]LRGP UMR 7274 CNRS-Université de Lorraine, ENSAIA, 2, avenue de la forêt de Hayes, 54500 Vandoeuvre-lès-Nancy, France

[‡]These authors contributed equally to this work

ABSTRACT

β-galactosidase (β-Gal) is one of the most important enzymes used in milk processing for improving their nutritional quality and digestibility. Herein, β-Gal has been entrapped into a meso-macroporous material (average pore size 9 and 200 nm, respectively) prepared by a sol-gel method from a silica precursor and a dispersion of solid lipid nanoparticles in a micelle phase. The physisorption of the enzyme depends on the concentration of the feed solution and on the pore size of the support. The enzyme is preferentially adsorbed either in mesopores or in macropores, depending on its initial concentration. Moreover, this selective adsorption, arising from the oligomeric complexation of the enzyme (monomer/dimer/tetramer), has an effect on the catalytic activity of the material. Indeed, the enzyme encapsulated in macropores is more active than the enzyme immobilized in mesopores. Designed materials containing β-Gal are of particular interest for food applications and potentially extended to bioconversion, bioremediation or biosensing when coupling the designed support with other enzymes.

1. Introduction

The use of enzymes as biocatalysts in industries, such as food[1], energy[2] or pharmaceutical synthesis[3] is increasing due to their high catalytic activity and selectivity. However, enzymes have a poor reusability and a low operational stability because of their sensitivity to pH and temperature. Immobilization of enzymes is one of the most promising methods to maintain enzyme performance when stability, recovery and reusability are targeted. Different immobilization strategies can be employed such as entrapment, microencapsulation, and cross-linked enzyme crystals (CLEC) or aggregates (CLEA)[4]. Methods based on physical adsorption, covalent attachment and affinity use a matrix, *i.e.*, a preexisting support for enzyme immobilization. The materials employed for such a purpose can be organic or inorganic. Investigating suitable solid supports in enzyme immobilization is still a current scientific challenge, depending on each specific enzyme and for each industrial application. The most common organic carriers are synthetic or natural polymers such as collagen, alginate, cellulose, chitosan and chitin. Standard inorganic materials are silica, celite, zeolites, glass and activated carbon[5]. Compared with organic resin supports, inorganic materials like silica offers special properties as immobilization supports such as high surface area, thermal stability, good mechanical properties, a low swelling in organic solvents while withstanding high flow rates in continuous reactors. It also exhibits a high biocompatibility, biodegradability and nontoxicity, and resistance to microbial attack.

Depending on the immobilization method, the chemical and physical properties of the enzyme can be altered. For example, through binding, the active conformation of an enzyme can be strongly modified, which in turn can lower its overall activity[6]. The physical adsorption of the enzyme can occur through weak forces such as hydrophobic interaction, hydrogen bonds, electrostatic and van der Waals forces.

Since their discovery in 1992[7], silica mesoporous materials have been widely used in enzyme immobilization due to their tunable pore size and volume and their large specific surface area. These materials can entrap a high amount of enzymes, and the immobilization results from either chemisorption or physisorption. Pores are a suitable environment for enhancing the thermal and pH stability of the enzymes as well as their resistance to high salt concentrations[8–10]. However, the confinement of the enzyme in pores[8] and/or a small pore size, or non-open-pore structures [10] can lead to a decrease of the enzymatic activity and might exhibit significant resistance to diffusion. By

increasing the pore size (e.g. from meso- to macropore sizes), one can expect an increase of the diffusion rates of substrates to the active sites of the enzyme and a higher enzyme mobility/flexibility within the cavities, resulting thus in a better enzyme activity[11]. Indeed, macroporous silica materials have a high mass transfer rate due to the interconnection of their broad pores, in addition to a good mechanical and thermal stability. However, even if the enzyme can be easily immobilized on this kind of materials, it can be also leached out easily, particularly when the pH of the media varies. To overcome this problem, the enzyme can be retained inside the material by crosslinking or by aggregation[12].

Hierarchical porous materials combine the properties of mesopores, such as high surface area and controllable pore size/volume, with those of macropores, providing high diffusion and throughput rates[13]. Although they are widely used in chemical catalysis[14], only a few examples have been reported in the literature for enzyme encapsulation. For instance, Cao et al[15] used hierarchical silica spheres to encapsulate glucose oxidase by physisorption. Meso-macroporous silica materials prepared by polycondensation of sodium silicate[11] were used to physisorb[11] and chemisorb β-galactosidase[16,17] and lipases[18–20]. Also, lipase was entrapped in solid lipid nanoparticles (SLN; W/O/W type) covered by a meso-macroporous silica shell[21] or covalently attached to a silica foam[22]. The fish-in-net technique was used to entrap various enzymes (umarase, trypsin, lipase, and porcine liver esterase) inside the macroporous cages while the mesopores provided a path for the diffusion of reactants[23]. Macro-mesoporous silica spheres prepared with a micro-device were used to covalently attach penicillin G acylase by grafting aminopropyl and glutaraldehyde[24]. Recently, catalase was used to prove the efficiency of hierarchical macro/mesoporous amino-grafted silica spheres as enzyme carriers[25].

In the present study, β-galactosidase (β-Gal) from *Kluyveromices lactis* was immobilized into hierarchical meso-macroporous silica by physical adsorption. The adsorption of the enzyme was investigated as a function of pore size and related to the specific activity within the material.

2. Materials and Methods

2.1 Materials

Cetyl palmitate (n-hexadecylpalmitate, NHP, >99% purity) and Pluronic® P-123, a non-ionic surfactant (Mn 5800 $g.mol^{-1}$), were purchased from Sigma-Aldrich (France). The tetramethoxysilane silica source (TMOS, 98% purity) was supplied by Alfa Aesar (Germany).

The β-Gal solution, extracted from *Kluyveromices Lactis*, EC 3.2.1.23, was kindly provided by Chr. Hansen holding company (Denmark) in a concentration of 25 mg of protein per mL of PEM buffer solution (prepared with Phosphate, Ethylenediaminetetraacetic acid and Magnesium, pH 6.5) and glycerol (1:1 w/w). The specific activity was determined spectrophotometrically from its ability to convert *o*-nitrophenyl-β-D-galactopyranoside (ONPG) into galactose and *o*-nitrophenol (ONP). For both free and immobilized enzyme, the activity was defined in international units (IU), 1 IU corresponding to the amount of enzyme catalysing the conversion of 1 μmol of ONPG per minute at 25°C. The reaction was carried out by mixing 0.5 mL of 40 mM ONPG and 0.5 mL of each enzyme solutions at 25°C, and run over 10 min. Adding 0.5 mL of 500 mM Na_2CO_3 solution stopped the reaction. The absorbance of ONP was measured at 420 nm (ε = 4.6 mM^{-1} cm^{-1}). The calculated specific activity of mother solution was 104 U mg^{-1} of enzyme (see Figure SI6). The enzyme was encapsulated without further purification.

2.2 Method for β-Gal immobilization

The physisorption of β-Gal in the porous silica material was carried out by gently stirring the samples for 48 h in a thermostatically controlled oven at 25°C. The samples were prepared by dispersing 25 mg of silica powder into 4 mL of PEM solutions (pH 6.5) containing various concentrations of enzyme, *i.e.* 1.25, 2.50, 12.5 and 25 $mg.mL^{-1}$. After immobilization, the resultant enzyme-loaded silica materials were washed 3 times with the PBS solution and centrifuged at 4000 rpm for 10 min. The final materials were labeled β-Gal_x@SiO_2, where x refers to the initial concentration of the enzyme solution used to load the silica materials.

2.3 Materials Characterization

Pore texture parameters of the bare and enzyme-loaded silica materials were derived from nitrogen adsorption isotherms at 77 K using a Micromeritics Tristar device. For

that purpose, all materials were degassed under vacuum over for 24 h at 20°C. The specific surface area (S_{BET}) was determined by applying the Brunauer-Emmett-Teller (BET) theory whereas pore volume and average pore size were obtained by application of the Barrett-Joyner-Halenda method (BJH) to the desorption branch of the isotherms.

Morphology and porosity of the bare silica material were observed by transmission electronic microscopy (TEM). The powder was first ground and then suspended in ethanol by sonication. A drop of the dispersion was spread out on the TEM carbon lacey grid and dried at room temperature before observation.

Zeta potential was measured using a Malvern Zetasizer 3000 HS instrument, based on 0.5 $mg.mL^{-1}$ suspension of bare or enzyme-loaded porous silica dispersed by sonication in aqueous solution at pH ranging from 2.5 to 9.

The mesoporous structure was also characterized by Small Angle X-ray Scattering (SAXSess mc^2, Anton Paar), operating with a CuKα radiation (λ = 0.1542 nm) at 40 kV and 50 mA with a line collimation setup. The signals were collected by a CCD camera and treated with the SAXSquant software. Powder samples were sandwiched in-between two Kapton® foils, and clamped in a steel sample holder. Diffraction data were recorded over 30 min exposure and corrected by subtracting the mica background.

Enzyme adsorption was quantified by thermogravimetric analysis (TGA) using a Netzsch STA 449F1 thermobalance. Approximately 10 to 15 mg of each sample were heated up to 800°C at 5 $°C.min^{-1}$ under air for the decomposition of organics.

Attenuated Total Reflectance Fourier Transformed InfraRed (ATR-FTIR) spectra were collected using a Lambda 1050 UV/VIS/NIR spectrophotometer (UltraViolet/VISible/Near InfraRed PerkinElmer device) with a diamond ATR crystal. The software for collecting and viewing spectra was the PerkinElmer UV WinLab. Each absorbance spectrum was obtained by accumulation of 32 scans at 4.0 cm^{-1} resolution using a clean ATR crystal exposed to the ambient atmosphere as a background. The spectra were collected with background corrections, and were plotted without further corrections. ATR-FTIR spectra were obtained using powdered samples.

2.4 Assay of β-Gal activity

The activity of the materials is the result of three assays. For the activity of the immobilized *β*-Gal, 1 mg of each powder of loaded silica materials was transferred into a tube containing 0.5 mL of buffer solution, to which 0.5 mL of 40 mM of ONPG

solution was subsequently added. The reaction was stopped after 10 min by adding 0.5 mL of 500 mM Na_2CO_3 solution. To remove the silica material, samples were centrifuged (4000 rpm during 30 sec) and the absorbance value of the ONP-containing supernatant was measured at 420 nm.

3. Results and discussion

3.1 Mechanisms of hierarchical meso-macroporous silica formation and enzyme loading

The meso-macroporous silica supports were thus obtained through a dual templating mechanism combining solid lipid nanoparticles and micelles of a block-copolymer surfactant used as templates for macropores and mesopores[21,26–28], respectively. The synthesis strategy is schematized in Figure 1. First, solid lipid nanoparticles of approximately 200 nm (as determined by dynamic light scattering (DLS), see supporting information, Figure S1) were formed in a micellar solution of Pluronic® P123 surfactant. A silica source, that hydrolyzed and polymerized around the colloidal template, was added to this dispersion to form a hybrid material. The as-obtained meso-macroporous material was then used to immobilize the *β*-Gal by dispersing the support in enzyme solutions of different concentrations (1.25, 2.50, 12.50 and 25.00 mg mL^{-1}).

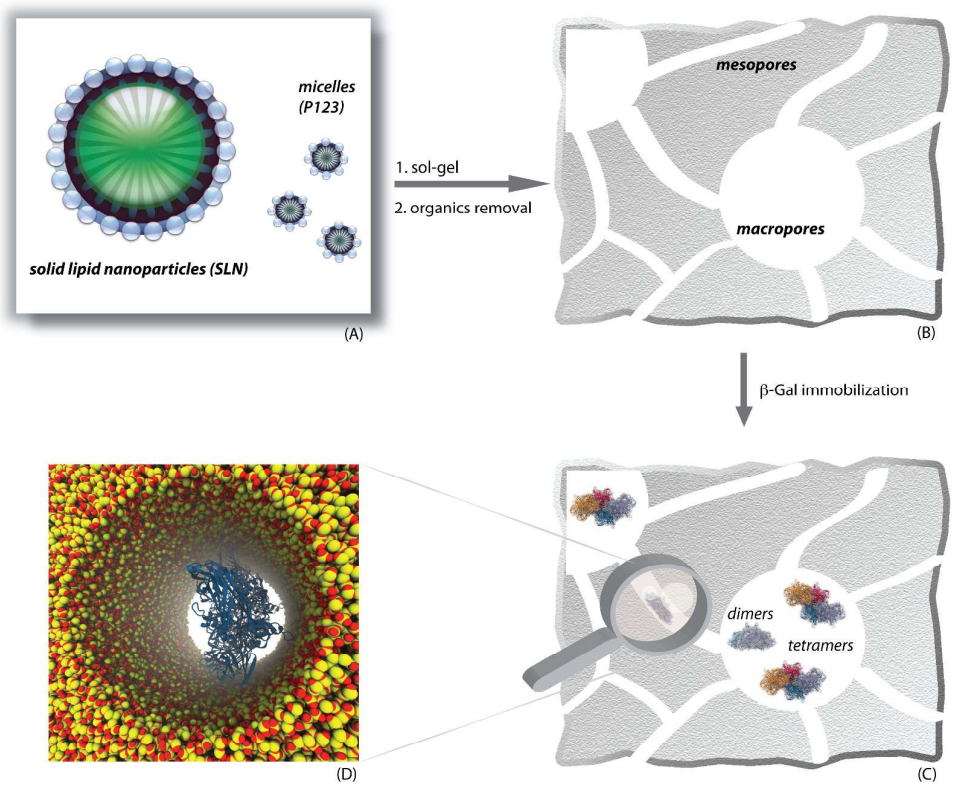

Figure 1. Schematic representation of the synthesis of meso-macroporous silica (A, B) and immobilization of *β*-Gal into meso and macropores (C, D).

3.2 Morphology and texture of bare and enzyme-loaded silica supports

TEM micrograph (Figure 2) of the silica support clearly shows a dual meso-macroporosity where the mesoporosity induced by the non-ionic surfactant is imprinted in the walls of the SLN-templated macropores.

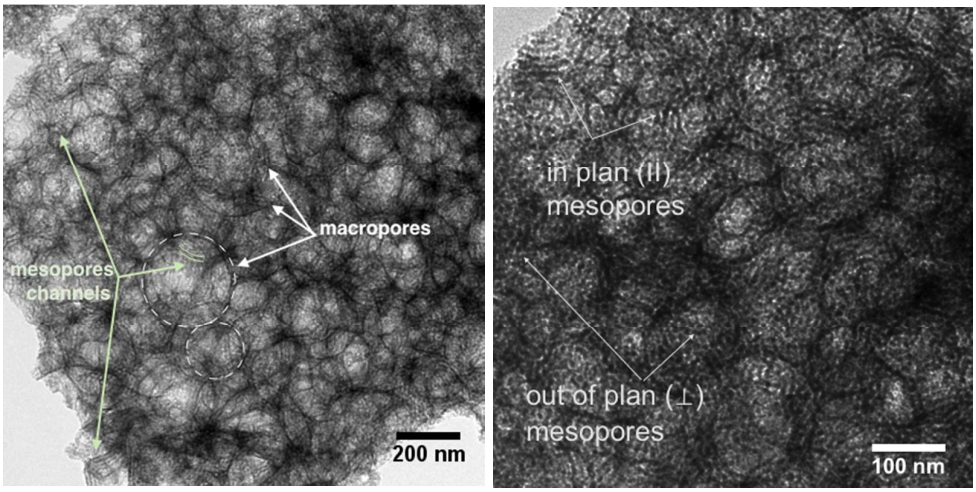

Figure 2. TEM pictures of bare silica material showing the mesopores network interconnecting macropores.

In agreement with TEM micrographs, the SAXS pattern of the bare SiO_2 material presented in Figure 3 confirmed the worm-like arrangement of mesopores with an average periodic Bragg distance (d_{Bragg}) of 12.4 nm. As for the enzyme-loaded silica, the intensity of the Bragg diffraction peaks decreased with the increase of the concentration of the feed solution from 1.25 to 12.50 mg mL^{-1}. As a matter of fact, when the mesoporosity is filled with organic molecules the scattering contrast consecutively decreases. Astonishingly, this progressive extinction of the Bragg peak stopped applying to the sample prepared at an enzyme concentration of 25.00 mg mL^{-1}, meaning that the corresponding material contained less β-Gal.

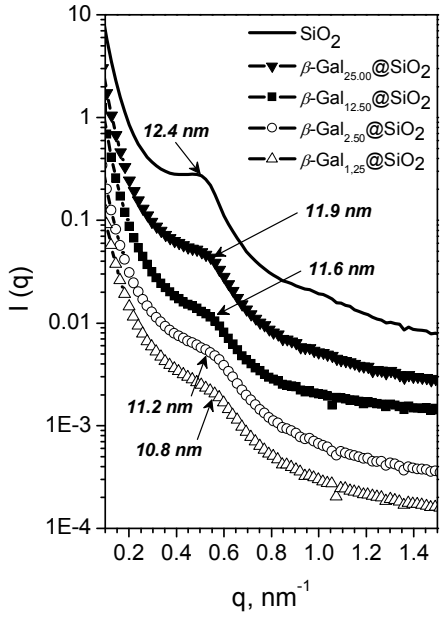

Figure 3. SAXS patterns of the bare and enzyme-loaded meso-macroporous silica support materials.

Nitrogen sorption measurements were performed on bare and enzyme-loaded silica materials as shown in Figure 4. Bare silica exhibited a type IV isotherm, characteristic of a mesoporous material. However, at high relative pressure (p/p_0 around 0.9), a steep increase of the values of adsorbed volume was observed, suggesting the presence of macropores and/or interparticular spaces. The pore size distribution obtained by the BJH method applied to the adsorption branch of the isotherm evidenced that the average mesopore size (Ø) was 9 nm for the bare silica. Moreover, the specific surface area (S_{BET}) and the pore volume (V_p) of the meso-macroporous bare material (SiO_2) were around 660 $m^2\ g^{-1}$ and 1.23 $cm^3\ g^{-1}$, respectively (see Table 1).

As expected, sorption data revealed that the values of S_{BET}, V_p and pore diameter of the *β*-Gal-loaded silica materials dramatically decreased with respect to bare silica. Upon increasing the initial concentration of the feed solution from 1.25 to 12.5 mg mL^{-1}, the specific surface area still decreased from 166 $m^2\ g^{-1}$ (for *β*-$Gal_{1.25}$ @SiO_2) to a threshold value of 85 $m^2\ g^{-1}$ on average (for *β*-$Gal_{2.50}$ @SiO_2 and *β*-$Gal_{12.50}$ @SiO_2). Likewise, for the same range of concentration, the pore volume values dropped by half from 0.26 $cm^3\ g^{-1}$ to a minimum average of 0.14 $cm^3\ g^{-1}$ while the pore diameter only slightly decreased, from 6.4 to 5.6 nm. This evolution of the texture parameters indicates that, in

the dilute regime, the enzyme uptake of the mesopores increased with the concentration of the feed solution. However, the material prepared with the most concentrated solution of 25.00 mg.mL^{-1}, β-Gal$_{25.00}$@SiO$_2$, presented significantly higher pore texture parameters with S_{BET}, V_p, and Ø of 239 cm^2 g^{-1}, 0.52 cm^3 g^{-1} and 6.8 nm, respectively. Those values remained lower than the ones of the bare silica, indicating that the enzyme was still physisorbed in the mesopores, but less than in the materials prepared with lower concentrations of enzyme.

A quantitative estimation of the variation of the silica wall thickness (ε) was made, by subtracting the pore diameters of each sample from the d_{Bragg} distances (see Table 1). A net thickening of the material wall (from 3.4 to 5.9 nm) was observed as soon as the bare material was loaded with a diluted feed solution, 1.25 mg mL^{-1} to 12.50 mg mL^{-1}. Then, just like for the other texture parameters, ε also decreased to 4.4 nm in the case of β-Gal$_{25.00}$@SiO$_2$ sample, indicating again a lower uptake of the enzyme in the mesopores when using higher enzyme feed solutions.

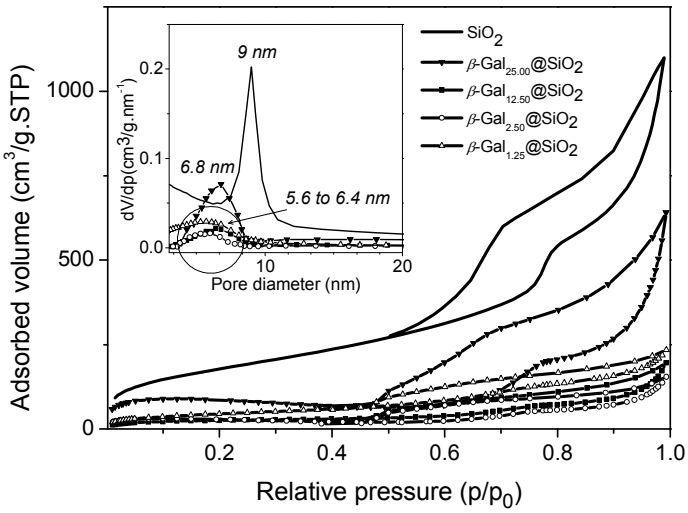

Figure 4. N_2 adsorption-desorption isotherms and corresponding pore size distributions.

Table 1. Parameters of bare and β-Gal-loaded meso-macroporous silica supports obtained from SAXS, nitrogen adsorption and thermogravimetric analysis. [a]Bragg distance determined by SAXS, [b]S_{BET}: specific surface area calculated from BET theory , [c]V_p : pore volume, [d]Ø : pore diameter, [e] wall thickness ($\varepsilon = d_{Bragg} - Ø$), [f]mass ratio, [g] Infrared band area ratio, [g]A_{amide}:A_{SiO2} : ratio of ATR peak areas.

	SAXS	*N_2 adsorption*				*TGA*	*ATR*
	d_{Bragg}[a] (nm)	S_{BET}[b] ($m^2\ g^{-1}$)	V_p[c] ($cm^3\ g^{-1}$)	Ø[d] (nm)	ε[e] (nm)	$m_{\beta\text{-Gal}}$: m_{SiO2}[f] (loading, wt%)	A_{amide}:A_{SiO2}[g]
SiO_2	12.4	657	1.23	9	3.4	0	0
β-$Gal_{1.25}$@SiO_2	10.8	166	0.26	6.4	5.1	1.17 (54)	0.11
β-$Gal_{2.50}$@SiO_2	11.2	80	0.12	5.6	5.6	1.45 (59)	0.15
β-$Gal_{12.50}$@SiO_2	11.6	90	0.17	5.7	5.9	1.55 (61)	0.13
β-$Gal_{25.00}$@SiO_2	11.9	239	0.52	6.8	4.4	0.84 (45)	0.05

N_2 adsorption measurements can only provide information on the enzyme presence in the mesopores. To get more information on the total enzyme loading in both mesopores and macropores, thermogravimetric analysis was performed (see Figure S2). The respective enzyme loading for each sample is presented in Table 1. It should be noted that the values of the β-Gal loading into those meso-macroporous silica materials are rather high compared to the one in organic resins[30] or hybrid materials[31]. The evolution of the loading values was in line with the trends previously observed by nitrogen sorption analysis and SAXS. Indeed, the β-Gal loading increased progressively in our case from 54 to 61wt% when the concentration of the enzyme solution increased from 1.25 to 12.5 mg mL^{-1}. But when enzyme adsorption was carried out at the highest concentration (25 mg mL^{-1}), β-Gal loading decreased down to 45wt%.

3.3. Interaction of β-Gal with meso-macroporous material

In order to investigate the interaction of the enzyme with the meso-macroporous silica material, zeta-potential measurements and ATR-FTIR analysis were performed. Zeta-potential measurements of bare and enzyme-loaded silica materials were carried out in water at different pH values. Figure 5 shows that the zeta-potential of the modified materials increased with the concentration of enzyme. At lower concentrations, the isoelectric point (pI) of the modified materials β-$Gal_{1.25}$@SiO_2 and β-$Gal_{2.50}$@SiO_2 was close to the pI of the bare silica material (2.5-3) and this might be explained by the presence of the enzyme mostly inside the silica mesoporous material. Indeed, no significant changes in the values of the zeta potential are observed meaning that the enzyme was not adsorbed on the external surface of the material. At higher

concentrations, the pI of the modified materials β-Gal$_{12.50}$@SiO$_2$ and β-Gal$_{25.00}$@SiO$_2$ increased to 4.2-4.5, *i.e.*, close to pI of the free enzyme, 5.42[32]. Therefore, it is reasonable to assume that the enzyme progressively filled the mesopores and then the macropores of the silica material.

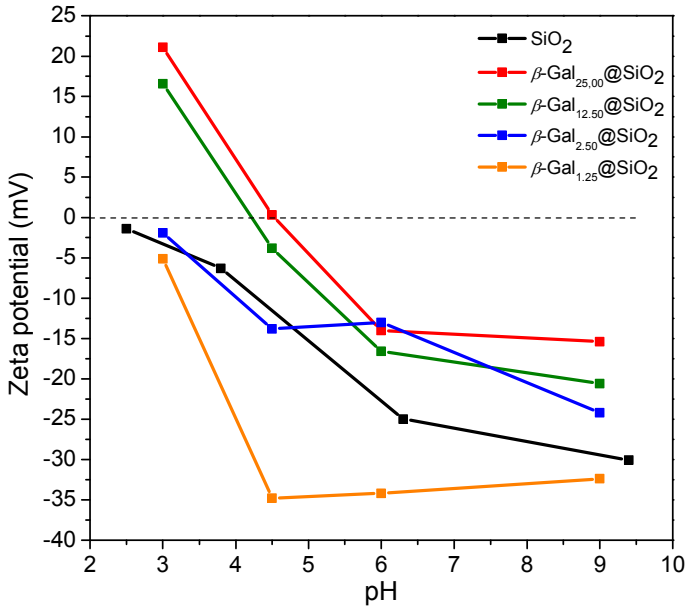

Figure 5. Zeta-potential measurements for the bare and the enzyme-loaded meso-macroporous silica.

On another hand, infrared experiments were carried out and the spectra are presented in Figure 6, without any correction. ATR-FTIR spectra of the bare material shows the typical bands of silica at 1065, 960 and 800 cm^{-1}, corresponding to Si-O-Si and Si-OH stretching vibrations.[33] After enzyme immobilization, the spectra exhibited a slight displacement of these bands (from 1065 to 1053 cm^{-1} and from 960 to 956 cm^{-1}, respectively), which can be attributed to the interactions between the enzyme and the silica support. The band at 1651 cm^{-1} (C=O stretching vibration) is characteristic of the amide I, whereas the band at 1535 cm^{-1} (N-H bending vibrations) is representative of the amide II. These bands are the consequence of the immobilization of β-Gal on the meso-macroporous silica by physical adsorption. In fact, other researchers have used these bands to characterize the presence of the enzyme adsorbed on the support.[34] All the spectra, including bare silica, showed some broad bands at around 2900 cm^{-1}, characteristic of C-H vibrations and related to the presence of the surfactant (Pluronic® P123), which was not completely removed after the Soxhlet extraction process. Indeed,

thermogravimetric analysis of the bare silica evidenced a mass loss of almost 21 wt.% that corresponds to the remaining surfactant (see Table 1). In agreement with the results obtained by TGA for the enzyme-loaded materials, one can also observe that the area ratios of the characteristic amide/silica bands (1651 cm^{-1} and 1058 cm^{-1}, respectively) followed the same trend as a function of the enzyme concentration in the feed solution (Table 1). When using diluted solutions to immobilize the enzyme inside the meso-macroporous silica material, the loading rate increased with the concentration from 1.25 to 2.5 mg mL^{-1}, and remained constant when increasing further the initial concentration of enzyme to 12.5 mg mL^{-1}. Interestingly, when directly immobilizing the enzyme from the stock solution at 25 mg mL^{-1}, the amount of encapsulated enzyme was lower. Thus, a selective adsorption occurred during the loading of the meso-macroporous silica material: (1) for diluted feed solution, the enzyme is preferentially physisorbed into mesopores and the loading rate is rather high (54-61wt%) and (2) for a concentrated feed solution, more enzyme located into macropores but the loading rate is smaller (45wt%).

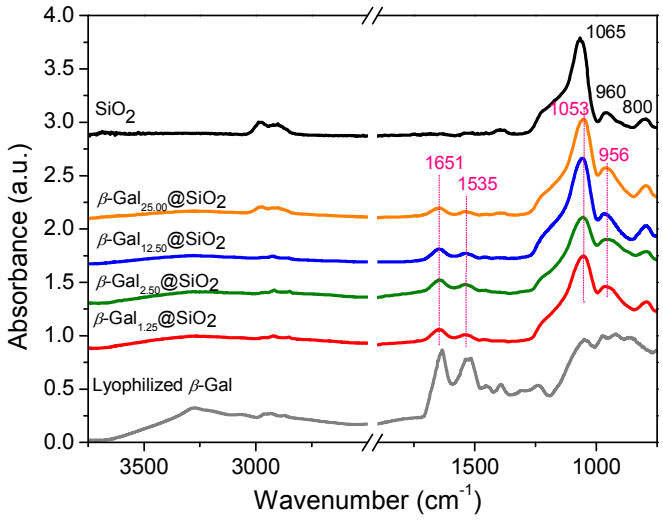

Figure 6. ATR-FTIR spectra of dried enzyme, bare silica, and meso-macroporous silica materials prepared at different feed solution concentrations.

In order to rationalize the physisorption mechanism of the enzyme into the meso-macroporous silica materials, the structure and the morphology of the enzyme was further considered. Using the molecular visualization program VMD[35], amino-acid distribution and geometrical sizes of *β*-Gal oligomers from *Kluyveromyces lactis* have been analysed based on the crystal structure reported previously by Pereira-Rodríguez et al.[36–38].Briefly, *β*-Gal forms a homo-oligomer of four subunits (A–B–C–D) that can be

described as a dimer of dimers. Each chain consists of 1024 residues with a molecular mass of 119 kDa. Monomers A–C and B–D form two identical dimers. The assembly of these dimers essentially occurs through interactions between monomers A and B, although there are also some contacts between monomers A and D, and monomers B and C that help stabilizing the tetramer. The dimer interfaces involve a significant proportion of hydrophobic interactions, whereas the tetramer interface results mostly from interactions between polar and/or charged residues (see Figure S3). As a consequence, the energy for dissociating the tertrameric assembly into two dimers is much lower (~ 6 kcal mol^{-1}) than the energy required to dissociate the dimer into two monomers (~ 20 kcal mol^{-1}).[39] In standard conditions, dimers and tetramers can definitely coexist and both exhibit an equal enzymatic activity.[40] The presence of silica can however displace the equilibrium between the two structural organizations.

The planar surfaces of the tetramer expose an excess of positively charged residues (~81 basic *vs* 73 acidic residues), as shown in Figure 7. Upon dissociation of the tetramer into two dimers, the solvent accessible surface area increases by 11% per dimer, and the number of accessible positively charged residues also steps-up. Thus, in the presence of negatively charged silanol groups, the equilibrium between the two oligomeric organizations is prone to be displaced toward the dimer.

Spatial extension of β-Gal *Kluyveromyces lactis* was inferred from the crystal structure of the tetramer (PDB 3OBA). Figures S4, S5 and S6 show that the tetramer, the dimer and the monomer can be contained in boxes of dimensions 15.1 nm × 17.1 nm × 10.7 nm, 11.9 nm × 15.6 nm × 7.2 nm, and 7.2 nm × 11.7 nm × 6.3 nm respectively. Size-wise, only the monomer and the dimer are susceptible to migrate into the mesopores of the hybrid silica material (measured average diameter of 9 nm), while the bulkier tetramer can only be physisorbed in macropores. Therefore, the following mechanism of the physisorption of the enzyme in the meso-macroporous silica material can be postulated: at low enzyme concentration, silica mesopores are progressively filled when increasing the concentration of the feed solution (from 1.25 to 12.5 mg mL^{-1}) with active dimers. However, when the feed solution reaches 25 mg·mL^{-1}, protein interactions leading to aggregation become important enough to limit or block the diffusion of the enzyme dimers in mesopores consistently with the lower uploading rate observed at high initial concentrations of the enzyme (see Figure 8).

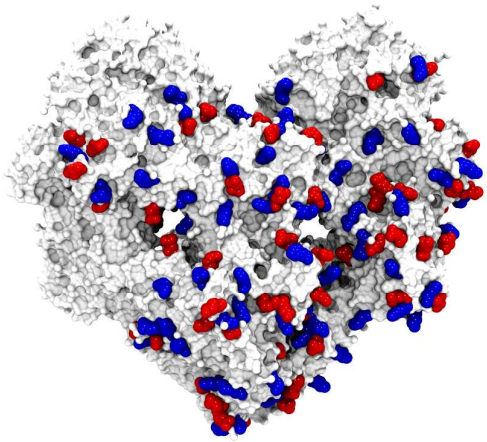

Figure 7. Acidic (red) and basic (blue) surface residues of β-Gal tetramer. Only residues having a Surface Accessible Solvent Area (calculated with a probe sphere radius of 0.14 nm) larger than 0.5 nm^2 are represented.

3.3. Activity of free and immobilized enzyme into meso-macroporous silica materials

In the investigated range of concentration, the activity of free β-Gal from *Kluyveromyces lactis* was independent of the enzyme concentration. Such an effect may be explained by both the absence of association and dissociation processes and by the specific activities of various oligomers at equilibrium being identical to each other. This behaviour was already observed with β-Gal from *Penicillium canescens* fungi, which also showed an equilibrium between monomers/dimers and tetramers, the active forms being dimers and tetramers[41]. The calculated specific activity of β-Gal was 104 U mg^{-1} of enzyme (see S7).

Upon physisorption in the meso-macroporous material, the enzyme specific activity depended on its location within the pores. When the enzyme was preferentially adsorbed (as dimers) in the mesopores, the specific activity increased with the increase of loading degree (Figure 8). This behaviour is often encountered for enzymes adsorbed within mesopores[42]. More interestingly, the specific activity of the enzyme physisorbed in the macropores was two times higher than that of the enzyme entrapped into mesopores. This might be due not only to the adsorption phenomenon but also to the increased release of the substrate.

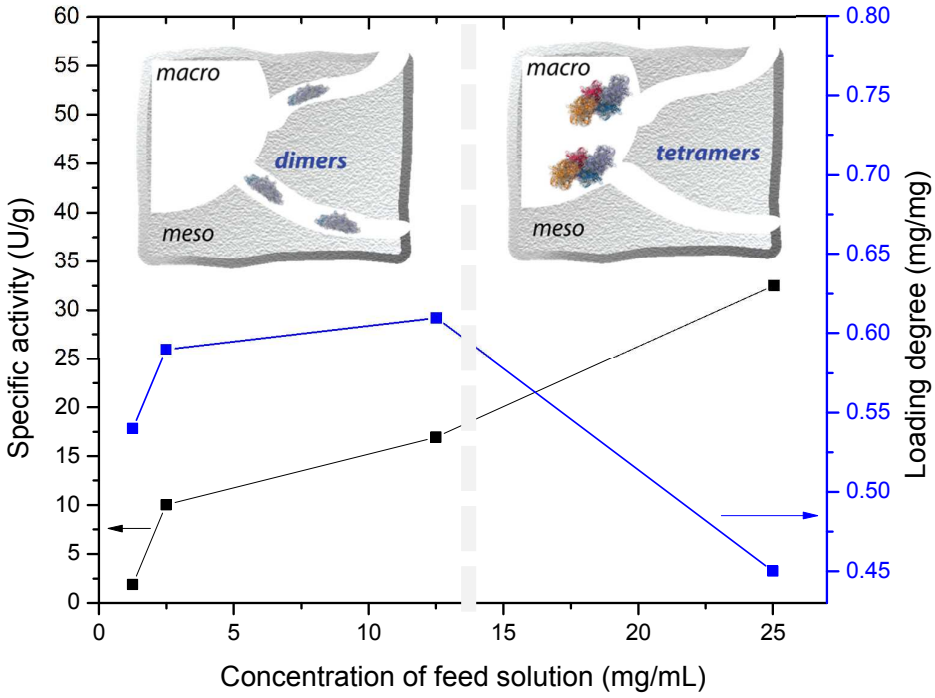

Figure 8. Evolution of the specific activity and loading degree showing the preferential adsorption of the enzyme either in mesopores (meso) or in macropores (macro), depending on the initial concentration.

Conclusion

In this study, *β*-Gal from *Kluyveromices lactis* was immobilized into hierarchical macro/mesoporous silica by physical adsorption. The support was obtained by a cooperative templating mechanism, using Pluronic® P123 micelles as porogen of mesopores on one hand, and a transcription mechanism using solid lipid nanoparticles templating macropores on the other hand. The enzyme was a tetramer, *i.e.*, a dimer of dimers with low dissociation energy in solution. The adsorption of enzyme at low concentrations in water took place preferentially in the mesopores as dimers or monomers, while the tetrameric form was adsorbed in the macropores. The enzyme immobilized in the macropores showed a higher specific activity than the one immobilized in the mesopores. Beyond food application, designed materials are of particular interest to bioconversion, bioremediation or biosensing when coupling the designed support with other enzymes.

Acknowledgements

The authors of this paper received funding from the People Program (Marie Curie Actions) of the European Union's Seventh Framework Program FP7/2007-2013/ under REA grant agreement n° 606713 BIBAFOODS. Authors thank Chr Hansen for providing the β-galactosidase enzyme and H. van den Brink and S. K. Dhayal for fruitful discussions. S. Prazeres is grateful to F. Guillén for his invaluable help in the activity studies. I.A. Pavel thanks S. Parant for technical assistance with UV and ATR-FTIR measurements.

Supporting Information. (1) preparation and characterization of solid lipid nanoparticles; (2) synthesis of meso-macroporous silica material; (3) thermogravimetry results of bare and loaded silica meso-macroporous materials; (4) views of X-ray crystal structure of β -Gal monomer, dimer and tetramer and (5) specific activity of β -Gal.

References

(1) Dale, D. *Microencapsulation in the Food Industry*; Elsevier, 2014.

(2) Fjerbaek, L.; Christensen, K. V; Norddahl, B. A Review of the Current State of Biodiesel Production Using Enzymatic Transesterification. *Biotechnol. Bioeng.* **2009**, *102* (5), 1298–1315.

(3) Pollard, D. J.; Woodley, J. M. Biocatalysis for Pharmaceutical Intermediates: The Future Is Now. *Trends Biotechnol.* **2007**, *25* (2), 66–73.

(4) Garcia-Galan, C.; Berenguer-Murcia, Á.; Fernandez-Lafuente, R.; Rodrigues, R. C. Potential of Different Enzyme Immobilization Strategies to Improve Enzyme Performance. *Adv. Synth. Catal.* **2011**, *353* (16), 2885–2904.

(5) Datta, S.; Christena, L. R.; Rajaram, Y. R. S. Enzyme Immobilization: An Overview on Techniques and Support Materials. *3 Biotech* **2012**, *3* (1), 1–9.

(6) Cao, L. Immobilised Enzymes: Science or Art? *Curr. Opin. Chem. Biol.* **2005**, *9* (2), 217–226.

(7) Beck, J. S.; Vartuli, J. C.; Roth, W. J.; Leonowicz, M. E.; Kresge, C. T.; Schmitt, K. D.; Chu, C. T. W.; Olson, D. H.; Sheppard, E. W.; McCullen, S. B.; et al. A New Family of Mesoporous Molecular Sieves Prepared with Liquid Crystal Templates. *J. Am. Chem. Soc.* **1992**, *114* (27), 10834–10843.

(8) Carlsson, N.; Gustafsson, H.; Thörn, C.; Olsson, L.; Holmberg, K.; Åkerman, B. Enzymes Immobilized in Mesoporous Silica: A Physical-Chemical Perspective. *Adv. Colloid Interface Sci.* **2014**, *205*, 339–360.

(9) Hudson, S.; Cooney, J.; Magner, E. Proteins in Mesoporous Silicates. *Angew.*

Chem. Int. Ed. Engl. **2008**, *47* (45), 8582–8594.

(10) Lee, C.-H.; Lin, T.-S.; Mou, C.-Y. Mesoporous Materials for Encapsulating Enzymes. *Nano Today* **2009**, *4* (2), 165–179.

(11) Bernal, C.; Sierra, L.; Mesa, M. Application of Hierarchical Porous Silica with a Stable Large Porosity for β-Galactosidase Immobilization. *ChemCatChem* **2011**, *3* (12), 1948–1954.

(12) Wang, M.; Qi, W.; Yu, Q.; Su, R.; He, Z. Cross-Linking Enzyme Aggregates in the Macropores of Silica Gel: A Practical and Efficient Method for Enzyme Stabilization. *Biochem. Eng. J.* **2010**, *52* (2–3), 168–174.

(13) Colombo, P.; Vakifahmetoglu, C.; Costacurta, S. Fabrication of Ceramic Components with Hierarchical Porosity. *Journal of Materials Science*. 2010, pp 5425–5455.

(14) Parlett, C. M. A.; Wilson, K.; Lee, A. F. Hierarchical Porous Materials: Catalytic Applications. *Chem. Soc. Rev. Chem. Soc. Rev* **2013**, *42* (42), 3876–3893.

(15) Cao, S.; Fang, L.; Zhao, Z.; Ge, Y.; Piletsky, S.; Turner, A. P. F. Hierachically Structured Hollow Silica Spheres for High Efficiency Immobilization of Enzymes. *Adv. Funct. Mater.* **2013**, *23* (17), 2162–2167.

(16) Bernal, C.; Sierra, L.; Mesa, M. Improvement of Thermal Stability of β-Galactosidase from Bacillus Circulans by Multipoint Covalent Immobilization in Hierarchical Macro-Mesoporous Silica. *J. Mol. Catal. B Enzym.* **2012**, *84*, 166–172.

(17) Bernal, C.; Urrutia, P.; Illanes, A.; Wilson, L. Hierarchical Meso-Macroporous Silica Grafted with Glyoxyl Groups: Opportunities for Covalent Immobilization of Enzymes. *N. Biotechnol.* **2013**, *30*, 500–506.

(18) Bernal, C.; Illanes, A.; Wilson, L. Heterofunctional Hydrophilic-Hydrophobic Porous Silica as Support for Multipoint Covalent Immobilization of Lipases: Application to Lactulose Palmitate Synthesis. *Langmuir* **2014**, *30* (12), 3557–3566.

(19) Guajardo, N.; Bernal, C.; Wilson, L.; Cabrera, Z. Selectivity of R-α-Monobenzoate Glycerol Synthesis Catalyzed by Candida Antarctica Lipase B Immobilized on Heterofunctional Supports. *Process Biochem.* **2015**, *50* (11), 1870–1877.

(20) Guajardo, N.; Bernal, C.; Wilson, L.; Cabrera, Z. Asymmetric Hydrolysis of Dimethyl-3-Phenylglutarate in Sequential Batch Reactor Operation Catalyzed by Immobilized Geobacillus Thermocatenulatus Lipase. *Catal. Today* **2015**, *255*, 21–26.

(21) Blin, J.-L.; Jacoby, J.; Kim, S.; Stébé, M.-J.; Canilho, N.; Pasc, A. A Meso-Macro Compartmentalized Bioreactor Obtained through Silicalization Of "green" double Emulsions: W/O/W and W/SLNs/W. *Chem. Commun. (Camb).* **2014**, *50* (80), 11871–11874.

(22) Brun, N.; Babeau-Garcia, A.; Achard, M.-F.; Sanchez, C.; Durand, F.; Laurent,

G.; Birot, M.; Deleuze, H.; Backov, R. Enzyme-Based Biohybrid Foams Designed for Continuous Flow Heterogeneous Catalysis and Biodiesel Production. *Energy Environ. Sci.* **2011**, *4* (8), 2840–2844.

(23) Yang, X. Y.; Li, Z. Q.; Liu, B.; Klein-Hofmann, A.; Tian, G.; Feng, Y. F.; Ding, Y.; Su, D.; Xiao, F. S. "Fish-in-Net" encapsulation of Enzymes in Macroporous Cages as Stable, Reusable, and Active Heterogeneous Biocatalysts. *Adv. Mater.* **2006**, *18* (4), 410–414.

(24) Zhao, J.; Wang, Y.; Luo, G.; Zhu, S. Immobilization of Penicillin G Acylase on Macro-Mesoporous Silica Spheres. *Bioresour. Technol.* **2011**, *102* (2), 529–535.

(25) Li, J.; Li, L.-S.; Xu, L. Hierarchically Macro/mesoporous Silica Sphere: A High Efficient Carrier for Enzyme Immobilization. *Microporous Mesoporous Mater.* **2016**, *231*, 147–153.

(26) Kim, S.; Stébé, M.-J.; Blin, J.-L.; Pasc, A. pH-Controlled Delivery of Curcumin from a Compartmentalized Solid Lipid Nanoparticle@mesostructured Silica Matrix. *J. Mater. Chem. B* **2014**, *2* (45), 7910–7917.

(27) Pasc, A.; Blin, J.-L.; Stébé, M.-J.; Ghanbaja, J. Solid Lipid Nanoparticles (SLN) Templating of Macroporous Silica Beads. *RSC Adv.* **2011**, *1* (7), 1204.

(28) Kim, S.; Diab, R.; Joubert, O.; Canilho, N.; Pasc, A. Core-Shell Microcapsules of Solid Lipid Nanoparticles and Mesoporous Silica for Enhanced Oral Delivery of Curcumin. *Colloids Surf. B. Biointerfaces* **2015**, *140*, 161–168.

(30) Gürdas, S.; Güleç H. A.; Mutlu M. Immobilization of *Aspergillus oryzae* β-Galactosidase onto Duolite A568 Resin via simple adsorption. *Bioprocess Technol* **2012**, *5* (3), 904-911.

(31) Jesionowski T.; Zdarta J.; Krajewska B. Enzyme immobilization by adsorption: a review. *Adsorption* **2014**, *20* (5), 801-821.

(32) Zhou, Q. Z. K.; Chen, X. D. Effects of Temperature and pH on the Catalytic Activity of the Immobilized [Beta]-Galactosidase from Kluyveromyces Lactis. *Biochem. Eng. J.* **2001**, *9* (1), 33–40.

(33) Launer, P. J.; Arkles, B. Infrared Analysis of Organosilicon Compounds:Spectra-Structure Correlations. *Silicone Compd. Regist. Rev.* **1987**, 100–103.

(34) Prazeres, S. F.; Ruiz, C. G.; García, G. M. Vibrational Spectroscopy as a Promising Tool to Study Enzyme-Carrier Interactions: A Review. *Applied Spectroscopy Reviews*. Taylor & Francis July 28, 2015.

(35) Humphrey, W.; Dalke, A.; Schulten, K. VMD: Visual Molecular Dynamics. *J. Mol. Graph.* **1996**, *14* (1), 33–38.

(36) Pereira-Rodríguez, Ángel Leiro, R. F.; Cerdán, M. E.; González Siso, M. I.; Fernández, M. B. Kluyveromyces Lactis β-Galactosidase Crystallization Using Full-Factorial Experimental Design. *J. Mol. Catal. B Enzym.* **2008**, *52–53*, 178–182.

(37) Pereira-Rodríguez, A.; Fernández-Leiro, R.; González Siso, M. I.; Cerdán, M. E.; Becerra, M.; Sanz-Aparicio, J. Crystallization and Preliminary X-Ray Crystallographic Analysis of Beta-Galactosidase from Kluyveromyces Lactis.

Acta Crystallogr. Sect. F. Struct. Biol. Cryst. Commun. **2010**, *66* (Pt 3), 297–300.

(38) Pereira-Rodríguez, A.; Fernández-Leiro, R.; González-Siso, M. I.; Cerdán, M. E.; Becerra, M.; Sanz-Aparicio, J. Structural Basis of Specificity in Tetrameric Kluyveromyces Lactis β-Galactosidase. *J. Struct. Biol.* **2012**, *177* (2), 392–401.

(39) Krissinel, E.; Henrick, K. Inference of Macromolecular Assemblies from Crystalline State. *J. Mol. Biol.* **2007**, *372* (3), 774–797.

(40) Becerra, M.; Cerdán, E.; Siso, M. I. G. Micro-Scale Purification of β-Galactosidase from Kluyveromyces Lactis Reveals That Dimeric and Tetrameric Forms Are Active. *Biotechnol. Tech.* **1998**, *12* (3), 253–256.

(41) Pilipenko, O. S.; Atyaksheva, L. F.; Poltorak, O. M.; Chukhrai, E. S. Dissociation and Catalytic Activity of Oligomer Forms of β-Galactosidases. *Russ. J. Phys. Chem. A* **2007**, *81* (6), 990–994.

(42) Lei, C.; Soares, T. a; Shin, Y.; Liu, J.; Ackerman, E. J. Enzyme Specific Activity in Functionalized Nanoporous Supports. *Nanotechnology* **2008**, *19* (12), 125102.

Table of contents (TOC)